MR Damper Identification using ANN based on 1-Sensor
A Tool for Semiactive Suspension Control Compliance

Juan C. Tudón-Martínez, Ruben Morales-Menendez, Ricardo A. Ramirez-Mendoza and Luis E. Garza-Castañón

Tecnológico de Monterrey, Av. E. Garza Sada 2501, 64849, Monterrey N.L., Mexico

Keywords: Magneto-Rheological Damper, Artificial Neural Networks, Semiactive Suspension Control.

Abstract: A model for a Magneto-Rheological (*MR*) damper based on Artifical Neural Networks (*ANN*) is proposed. The *ANN* model does not require regressors in the input and output vector, i.e. is considered static. Only one sensor is used to achieve a reliable *MR* damper model which is compared with experimental data provided from two *MR* dampers with different properties. The *RMS* of the error is used to measure the model accuracy; from both *MR* dampers, an average value of 7.1% of total error in the force signal is obtained by taking into account 5 different experiments. The *ANN* model, which represents the nonlinear behavior of an *MR* damper, is used in a suspension control system of a Quarter of Vehicle (*QoV*) in order to evaluate the comfort of passengers maintaining the road holding. A control technique with the *MR* damper model is compared with a passive suspension system. Simulation results show the effectiveness of a semiactive suspension versus the passive one. The *RMS* of the comfort signal improves 7.4% with the *MR* damper while the road holding gain in the frequency response shows that the safety in the vehicle can be increased until 40.4% with the semiactive suspension system. The accurate *MR* damper model validates a realistic *QoV* response compliance.

1 INTRODUCTION

A Magneto-Rheological (*MR*) damper is an hydraulic damper whose oil contains metallic particles that change the rheological properties (i.e. viscosity) of the fluid when a magnetic field is applied; an electric current supplied through the damper coil is used to manipulate the magnetic phenomenon. The variation of the oil viscosity allows to modify the damping ratio in the shock absorber, this property is named *semiactivity*. The oil viscosity is proportional to the electric current as well as to the *MR* damper force; however, the join of these mechanisms creates an highly nonlinear behavior in the damping force. The *MR* damper has been mainly applied in vibration control because it has low power requirement, fast response, simple structure and continuous adjustable damping force over a large span.

The main function of the *MR* damper in an automotive suspension is to absorb energy in order to get low accelerations of the sprung mass (i.e. automotive chassis) and low deflections in the wheel; thus, an accurate *MR* damper model is required to design the control system. Even there are important contributions in this field (Guo et al., 2006); there are still several needs. Figure 1 shows the highly nonlinear behavior of an industrial *MR* damper under various constant electric current inputs, its accurate modeling is a non-trivial task.

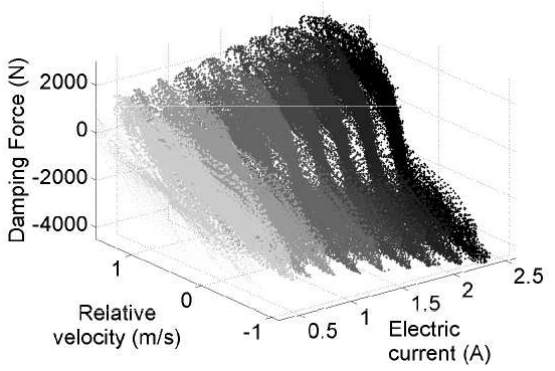

Figure 1: Nonlinear behavior of the *MR* damper force respect to the control current and relative velocity.

Several mathematical models are available for modeling the nonlinear behavior of *MR* dampers; generally, they can be grouped as parametric and non-parametric models. Parametric models include the Bingham model (Stanway et al., 1987),

C. Tudón-Martínez J., Morales-Menendez R., A. Ramirez-Mendoza R. and E. Garza-Castañón L..
MR Damper Identification using ANN based on 1-Sensor - A Tool for Semiactive Suspension Control Compliance.
DOI: 10.5220/0004159004930502
In *Proceedings of the 4th International Joint Conference on Computational Intelligence* (NCTA-2012), pages 493-502
ISBN: 978-989-8565-33-4

the viscoelastic-plastic model (Gamota and Filisko, 1991), the phenomenological model (Wang and Kamath, 2006), the semi-phenomenological model based on the BoucWen model (Spencer et al., 1996), the improved BoucWen model (Yang et al., 2002), the hyperbolic tangent function model (Kwok et al., 2006), (Guo et al., 2006), the inverse tangent function model (Çesmeci and Engin, 2010) and many others. The Bingham and the viscoelastic-plastic model can not reproduce the nonlinear behavior of an *MR* damper with high accuracy, while the other models can; however, they have many parameters to identify. On the other hand, some of these physical models use parameters of the internal structure of the shock absorber resulting a particular model case.

In the non-parametric models, the coefficients do not have a physical meaning. Models based on look-up table, fuzzy logic and Artificial Neural Networks (*ANN*) are the representative non-parametric models for a *MR* damper. Polynomial models [(Choi et al., 2001), (Hong et al., 2002), (Du et al., 2005), (Poussot-Vassal et al., 2008)] require many parameters to express the nonlinear and semiactive behavior of the damping force; while the fuzzy models [(Atray and Roschke, 2003), (Ahn et al., 2008)] need a priori knowledge in the frequency and time domain of the *MR* damper. For *ANN* models, the knowledge of the dynamic relationships between the variables is not required, only a well training step is needed; in addition, the number of parameters depends on the structure size and commonly the *ANN* design is based on the minimal dimensions criterion (Freeman and Skapura, 1991), which selects the possible lowest number of hidden layers with the possible lowest number of neurons.

The major effort in the *MR* damper modeling, by using *ANN*, is focused on reproduce the inverse dynamics (force-electric current) of the shock absorber (Chang and Zhou, 2002), (Zapateiro et al., 2009), (Metered et al., 2010); however, a recurrent neural network is required for achieving an optimal damping force signal, and normally the input vector is based on two or more sensor measurements: force, displacement and/or velocity. This type of *ANN* model increases the architecture size and the instrumentation cost in a suspension control system. On the other hand, commonly the modeling of the forward dynamics using *ANN* requires two ore more time delays of each input by increasing the *ANN* architecture and its computing time (Savaresi et al., 2005), (Chen et al., 2009), (Boada et al., 2011).

This paper proposes a non-parametric model of an *MR* damper based on *ANN*, the model does not require regressors in the input vector and demands only one sensor, i.e. its structure has low complexity for practical implementations of suspension control systems. The *MR* damper model is validated with experimental data of two *MR* dampers for analyzing its reliability and it is used in a suspension control system of a Quarter of Vehicle (*QoV*), this is an example of an application problem where the accurate modeling of the actuation device is one of the most crucial part of the whole control design problem.

The outline of this paper is as follows: in the next section, the *ANN* design is described. Section 3 shows the experimental system and section 4 presents the modeling results. Section 5 presents the effectiveness of an *MR* damper versus a passive damper in compliance of a suspension control system. Conclusions are presented in section 6.

Table 1: Definition of variables.

Variable	Description
F_{MR}	*MR* damper force
z_{def}	Damper piston position
$\dot{z}_{def}$	Damper piston velocity
I	Electric current
k_i	Time delays
m_s	Sprung mass in the *QoV*
m_{us}	Unsprung mass in the *QoV*
z_r	Road profile
z_s	Vertical position of m_s
z_{us}	Vertical position of m_{us}
$\dot{z}_s$	Vertical velocity of m_s
$\dot{z}_{us}$	Vertical velocity of m_{us}
$\ddot{z}_s$	Vertical acceleration of m_s
$\ddot{z}_{us}$	Vertical acceleration of m_{us}
k_s	Spring stiffness coefficient
k_t	Wheel stiffness coefficient

2 ANN REVIEW

An *ANN* is a computational model capable to learn behavior patterns of a process, it can be used to model nonlinear, complex and unknown dynamic systems, (Korbicz et al., 2004). Based on the flow of signals, the *ANN* architecture can be classified into two major groups: *feedforward* and recurrent networks. *Feedforward* networks project the flow of information only in one way, i.e. the output of a neuron feeds to all neurons of the following layer (Hagan et al., 1996); while, the recurrent networks have an output feedback signal.

In *MR* damper modeling using *ANN*, typically recurrent neural networks based on Nonlinear-ARX (*NARX*) structures, i.e. regressors in the input and/or output vector, have been proposed with high accuracy (Chang and Zhou, 2002), (Savaresi et al., 2005), (Zap-

ateiro et al., 2009), (Chen et al., 2009), (Metered et al., 2010), (Boada et al., 2011). The *NARX* structure is defined as,

$$F_{MR} = f_{NL}(z_{def}(t), z_{def}(t-1), \ldots, z_{def}(t-k_1), \dot{z}_{def}(t), \dot{z}_{def}(t-1), \ldots, \dot{z}_{def}(t-k_2), I(t), I(t-1), \ldots, I(t-k_3), F_{MR}(t-1), \ldots, F_{MR}(t-k_4)) \quad (1)$$

where k_i represents a specific number of time delays for each signal, z_{def} and $\dot{z}_{def}$ are the displacement and velocity of the damper rod provided from sensor measurements, I is the actuation signal and F_{MR} is the damper force (*ANN* output).

In this paper, a comparison between a *feedforward* and recurrent neural network is considered for determining the accuracy degree in the damper force by adding the output feedback in the *ANN* structure. In addition, different arrays in the input vector are used to evaluate the *ANN* performance with time delays; the arrays with one, two and three regressors in the input vector are compared with the modeling performance of an *ANN* that does not have delays. Finally, the *ANN* performance is analyzed when one (velocity) or two (displacement and velocity) signals are used in the input vector.

The *ANN* training is defined as the adaptation process of the synaptic connections under external stimulations. The *backpropagation* algorithm is the most used training method since it allows to solve problems with complex net connections; its formulation can be reviewed in detail in (Freeman and Skapura, 1991). The proposed *ANN* model was trained with *backpropagation* and crossed validation was used to validate the results.

3 EXPERIMENTAL SYSTEM

Two different *MR* dampers have been used to perform a total of 5 tests. One damper, called MR_1 damper, is designed by Delphi MagneRide^{TM}; it has continuous actuation and considerable hysteresis at high frequencies with high deflections. The other *MR* damper, named MR_2 damper, is manufactured by BWI^{TM}; it has only two levels of actuation and its hysteretic behavior is minimal.

An MTS-407^{TM} controller has been used to control the position of the damper piston, Figure 2. An NI-9172^{TM} data acquisition system commands the controller and records the position, velocity and force from the *MR* damper. A sampling frequency of 1650 Hz was used. The bandwidth of displacement was 0.5- 15 Hz, which lies within comfort and road holding automotive applications. The displacement and electric current ranges were: $\pm$25 mm and 0 - 2.5 A, respectively.

Figure 2 also shows the used sensor (VP510-10 of UniMeasure^{TM}), which provides the velocity ($\dot{z}_{def}$) and position (z_{def}) measurements of the damper piston. In this case, a self-generating tachometer generates the velocity measurement; however, it is possible to use another linear velocity transducer.

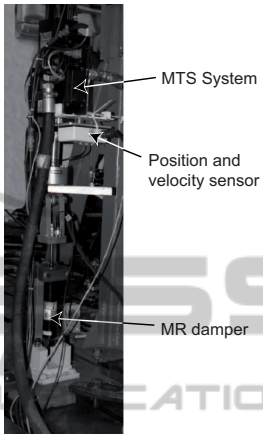

Figure 2: Experimental system.

A series of training sequences have been proposed in (Lozoya-Santos et al., 2009), the position emulates the suspension deflection and the electric current is the actuation signal. Table 2 shows the design of experiments used to identify the nonlinear behavior of both *MR* dampers under different sequences of position and actuation.

For displacement sequences, Amplitude-Modulated (*AM*), Frequency-Modulated (*FM*) and Stepped Frequency Sinusoidal (*SFS*) were used to analyze the *MR* damper dynamics in the transient response under changes in magnitude and frequency of the suspension deflection; Triangular wave with Positive and Negative Variable Slopes (*TPNVS*) sequence allows to know the dynamic behavior under constant velocity; and Road Profile (*RP*) represents the suspension deflection move when the vehicle passes under a specific surface. Figure 3 presents some of the different displacement sequences used in the experimental stage in order to identify the nonlinear behavior of both *MR* dampers.

For electric current sequences, Stepped inCrements (*SC*) are used to study the effect of the current in the jounce and rebound of the *MR* damper under different displacements, since the MR_2 damper has not a continuous actuation only two levels of current were designed; Increased Clock Period Signal (*ICPS*) and Pseudo Random Binary Signal (*PRBS*) allow to analyze the transient response of the damping force

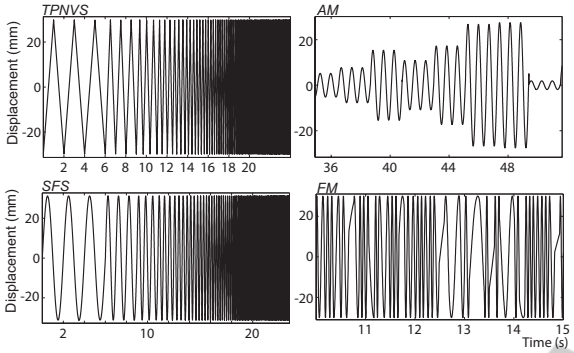

Figure 3: Displacement sequences in the piston used in the experimental stage.

when the current changes at different frequencies, the *ICPS* signal includes random changes in the amplitude and *PRBS* only switches between two electric current values. Figure 4 shows the behavior of the actuation sequences used in the experiments, for the MR_2 damper, the *SC* sequence only has two states: 0 and 2.5 A.

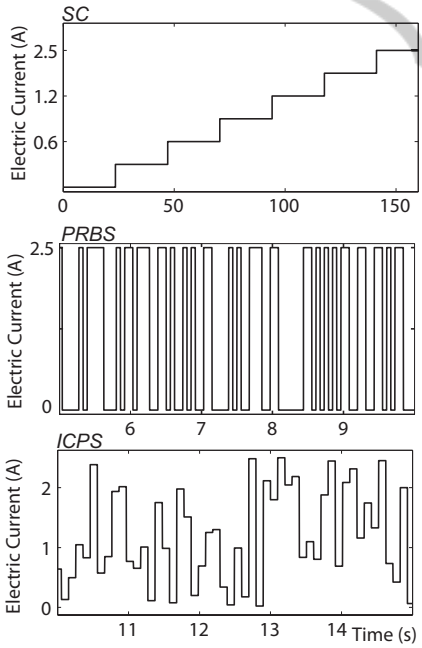

Figure 4: Electric current sequences used in the experimental stage.

4 MODELING RESULTS

The *ANN* model obtained from the different experiments, presented in Table 2, is used to characterize the dynamical behavior of the *MR* damper and evaluated by the Root Mean Square (*RMS*) performance

Table 2: Design of experiments for identifying an *MR* damper.

Experiment	Displacement sequence	Current sequence	
		MR_1	MR_2
1	*TPNVS*	*SC* (10)	*SC* (2)
2	*SFS*	*SC* (10)	*SC* (2)
3	*RP* (rough way)	*ICPS*	*PRBS*
4	*AM*	*ICPS*	*PRBS*
5	*FM*	*ICPS*	*PRBS*

index of the error, which is defined as,

$$RMS = \sqrt{\frac{\sum_{i=1}^{n}\left(\hat{F}_{MR}(i) - F_{MR}(i)\right)^2}{n}} \qquad (2)$$

where, $\hat{F}_{MR}$ and F_{MR} represent the estimated and experimental damping force respectively and n is the number of total samples in the experiment. The percentage of error represents the *RMS* of the error normalized by the span of the damping force.

First, the design issues for the *ANN* model are discussed: the network structure, the required sensors in the input vector, the regressor choice and the selection of the number of parameters of the *ANN*.

Remark: *ANN* architecture. A Multilayer Perceptron (*MLP*) network, which corresponds to a *feedforward* system, is compared with a recurrent network. The input vector of the *MLP* network is composed by z_{def}, $\dot{z}_{def}$, I; while the recurrent network adds the *ANN* output (damping force). Table 3 presents the modeling error of both structures by using the experiment 2 in the MR_1 damper as example. The error percentage represents the average deviation between the modeled damping force and the real measurement based on the *RMS* value of the error. When the feedback of the *MR* damper force is considered, the modeling error decreases slightly; however, the *ANN* architecture and its computing time increase.

Table 3: Performance comparison between the *feedforward* and recurrent neural networks.

ANN Structure	Error (%)
MLP (*feedforward*)	4.38
Recurrent	3.80

Remark: Sensors in the Input Vector. Taking into account an *MLP* network, two different input vectors have been compared. The former input vector uses the z_{def}, $\dot{z}_{def}$ and I; while the second one only includes $\dot{z}_{def}$ and I. Table 4 indicates that the modeling error decreases 46.7 % by considering two sensor measurements in addition to the electric current signal; however, the instrumentation cost can increase and the *ANN* structure is more complex for the training and testing step.

Table 4: Modeling error (%) in the *MLP* network using different input vectors.

Sensor Measurements	Error (%)
1 ($\dot{z}_{def}$)	8.22
2 (z_{def} and $\dot{z}_{def}$)	4.38

Remark: Regressor Choice. Once the *ANN* architecture and the input vector are defined, different arrays in the input vector of the *ANN* model have been evaluated, in this case the experiment 2 over the MR_1 damper is used as example. Table 5 shows the modeling error of the *ANN* when the number of regressors in the 2 input signals varies; in this analysis, the velocity and electric current have the same number of regressors in each test. According to the modeling error, it is not significant to incorporate time delays in the input vector of the *ANN*.

Table 5: Modeling error (%) in the *ANN* with different number of regressors in the input vector.

Regressors	Error (%)
0	8.22
1	8.24
2	8.86
3	8.79

Remark: *ANN*-size Selection. Finally, the choice of the number of parameters (hidden layers and neurons in these layers) of the non-linear parametric function can be easily made using a cross-validation approach. A 1-hidden-layer structure has been chosen by simulation tests, this structure guarantees the universal-approximation property (Sjöberg, 1995). For determining the number of neurons in the hidden layer, the minimal dimensions criterion is used (Freeman and Skapura, 1991); the best choice is with 10 neurons.

According to the above design issues, the *ANN* architecture used to model the *MR* damper dynamics is (2,10,1), Figure 5. The *ANN* input vector includes the signal of the relative velocity and the excitation signal (electric current) without considering regressors, while the damping force corresponds to the *ANN* output. Modeling results of the proposed *ANN* model, considering the 5 experiments, is shown in the Table 6. Figure 6 shows the variability of the modeling results. Clearly, the variance of the error is greater in the model of the MR_1 damper since its continuous actuation adds more nonlinearities, which complicate the modeling task; while, the MR_2 damper model shows better modeling performance with lower error standard deviation of the error.

The *RMS* average, considering all experiments, is 291.4 N for the MR_1 damper and 597.8 N for the MR_2 damper. Since the span of the force is $\pm$4000 N approximately for the MR_1 damper and [$-$6000 to 11000] N for the MR_2 damper, the obtained *RMS* average represents the 7.25% and 7.02% of punctual error in the force signal, respectively. Figure 7 presents a qualitative comparison in the transient response of the force obtained from experimental data and from *ANN* model; in this case, the MR_1 and MR_2 dampers are subject to the experiment 5. According to Table 6, the MR_1 damper has greater modeling error in the experiment 2 and 5, and viceversa.

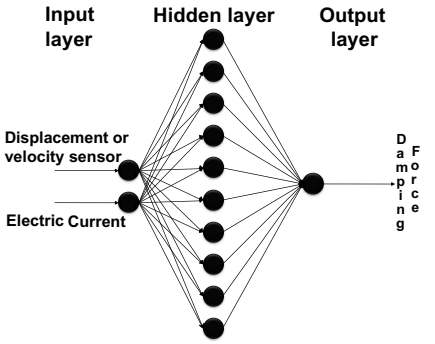

Figure 5: Feedforward *ANN* of the *MR* damper model.

Table 6: Modeling error in different experimental tests.

MR damper	Experiment				
	1	2	3	4	5
MR_1	5.9%	8.2%	3.1%	4.1%	14.95%
MR_2	6.9%	6.8%	7.2%	8.0%	6.2%

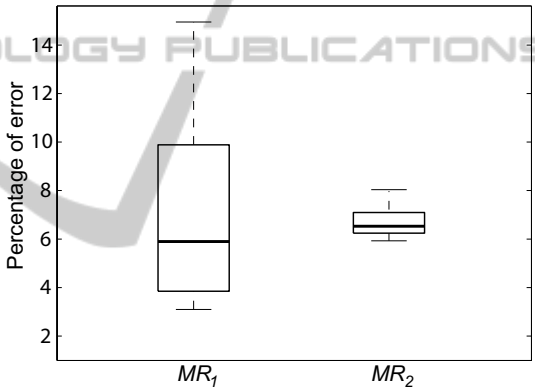

Figure 6: Variability of the error in the *MR* damper models.

In order to test the capability of the *ANN* for modeling the nonlinear and hysteretic behavior of the *MR* damper, experimental data are compared with the *ANN* model in the characteristic diagram of Force-Velocity (*FV*); this diagram explains the effect of jounce and rebound of the damper and it is a tool for the engineers of automotive design in order to define the suspension capability for improving the confort and road holding. Figure 8 shows the *FV* diagram of

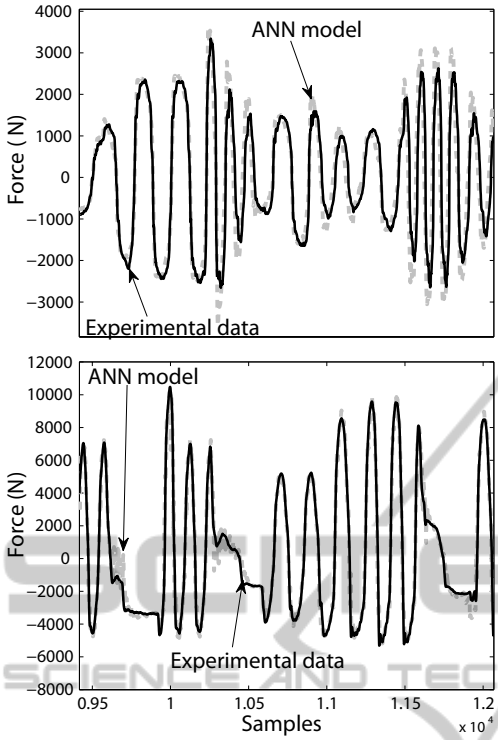

Figure 7: Comparison between the real and modeled force using the MR_1 damper (up) and MR_2 damper (bottom).

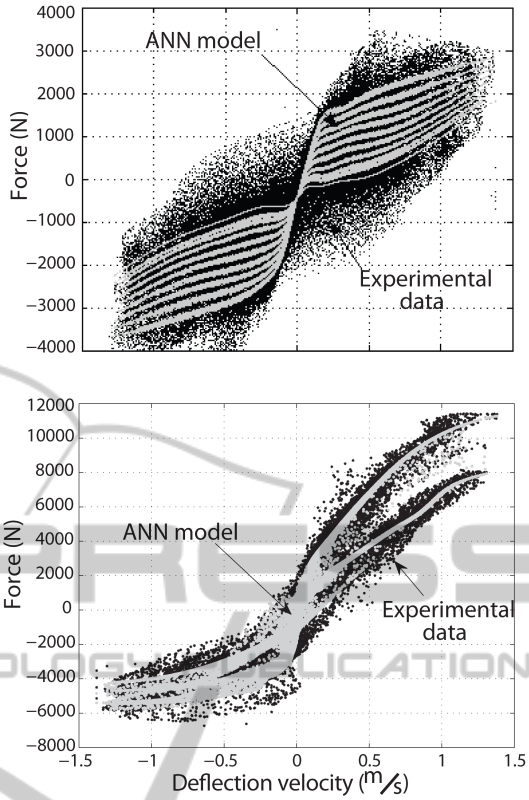

Figure 8: *FV* diagram for the real and modeled force using the MR_1 damper (up) and MR_2 damper (bottom).

both dampers using the experiment 2. Bottom plot in Figure 8 shows that the *ANN* can model the nonlinear behavior of the MR_2 damper with acceptable accuracy, only outliers are not included. Notice in the *FV* diagram that the MR_2 damper has minimal hysteresis and it is composed by two damping leves: 1) high damping force at current greater than 2.5 A and 2) low damping force at 0 A. On the other hand, the MR_1 damper has a continuous actuation between 0 and 2.5 A. The *ANN* correctly models the nonlinear behavior at each current step; however, the hysteresis can not be modeled at low deflection velocities ($\pm$0.5 m/s) using only one sensor, up plot in Figure 8. This hysteretic behavior occurs at high frequencies (greater than 10 Hz) with high amplitudes in the suspension deflection, and the velocity sensor does not contain the required information for representing the force dynamics at these frequencies; thus, an acceleration sensor could complement this missing force dynamics.

Although the hysteresis can not be modeled at high frequencies with high displacements, in general, the proposed *ANN* can be used to represent the *MR* damper dynamics since the hysteretic behavior appears at not typical deflection amplitudes in an automotive suspension and the frequencies out of the desired span for passengers comfort, i.e. the position pattern is out of the automotive operational zone of the damper. Figure 9 shows the comparison of the *FV* diagram using experimental data provided from the experiment 2 (left plot) and 4 (right plot). Since the experiment 4 contains data at high frequencies but low amplitudes on the displacement, the hysteresis phenomenon is minimal; while, the experiment 2 has high displacements at high frequencies that cause too much hysteresis.

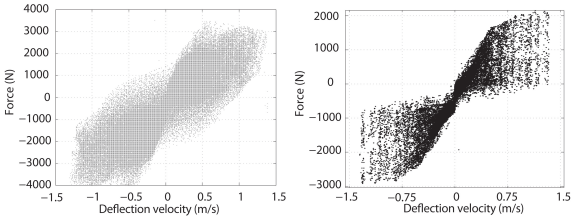

Figure 9: *FV* diagram for the MR_1 damper using experimental data from experiment 2 (left) and 4 (right).

Another form of getting the *ANN* model of the *MR* damper is by using the estimated deflection velocity through a displacement sensor. Figure 10 shows that the measurement of the deflection velocity is prac-

tically similar to the estimated signal, in this case the central differentiation algorithm over the displacement measurement is considered. Therefore, it can be used a displacement or velocity sensor, additional to the actuation signal, for achieving a reliable *MR* damper model based on *ANN*.

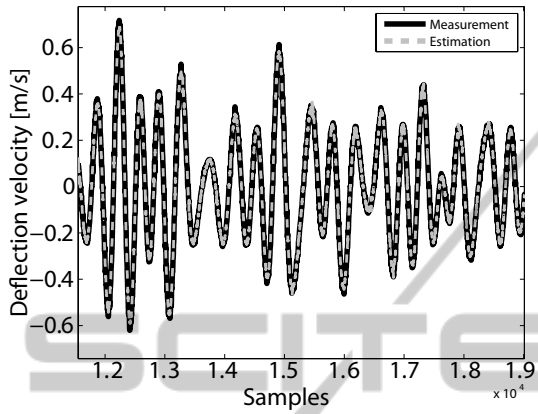

Figure 10: Comparison between the real and estimated deflection velocity for the experiment 3 in the MR_2 damper.

5 MR DAMPER USED IN AUTOMOTIVE SUSPENSIONS

In order to analyze the effectiveness of the *MR* damper model based on *ANN*, a semiactive suspension control system of a *QoV* model is used as testbed; the *ANN* model is included for increasing the comfort of passengers maintaining the road holding.

The *QoV* model considers a sprung mass (m_s) and an unsprung mass (m_{us}). A spring with stiffness coefficient k_s and a *MR* damper represent the suspension between both masses. The stiffness coefficient k_t models the wheel tire. The vertical position of the mass m_s (m_{us}) is defined by z_s (z_{us}), while z_r corresponds to the road profile. It is assumed that the wheel-road contact is ensured.

The system dynamics is given by,

$$m_s\ddot{z}_s = -k_s(z_s - z_{us}) - F_{MR} \quad (3)$$

$$m_{us}\ddot{z}_{us} = k_s(z_s - z_{us}) - k_t(z_{us} - z_r) + F_{MR} \quad (4)$$

where, F_{MR} is the *MR* damping force obtained by the *ANN* model, which is based on the MR_2 damper dynamics. The *QoV* model parameters described in 3 and 4 have been identified on a commercial vehicle, Table 7.

The *MR* force depends on the deflection velocity $\dot{z}_{def} = \dot{z}_s - \dot{z}_{us}$ and electric current I, this later signal represents the controller output. Several approaches

Table 7: *QoV* model parameters of a commercial vehicle.

Parameter	Value
m_s	387 (Kg)
m_{us}	139.5 (Kg)
k_s	37,300 (N/m)
k_t	295,200 (N/m)

in control of semiactive suspensions have been proposed (Dong et al., 2010), (Spelta et al., 2010), etc.

The comfort performance of a semiactive suspension, using the Mix 1-sensor (*Mix*1) control law, is compared with a commercial vehicle suspension which uses a passive damper. Experimental data of the passive damper were modeled by the same *ANN* technique as the semiactive dampers. Figure 11 shows a conceptual diagram of the semiactive suspension control system; the *ANN* model, which has been trained off-line, only requires the deflection velocity and the electric current for generating the *MR* force in a forward way. The block of processing of signals includes filters, estimators and/or observers in order to achieve the control law. Details on the *Mix*1 control law can be reviewed in (Spelta et al., 2010).

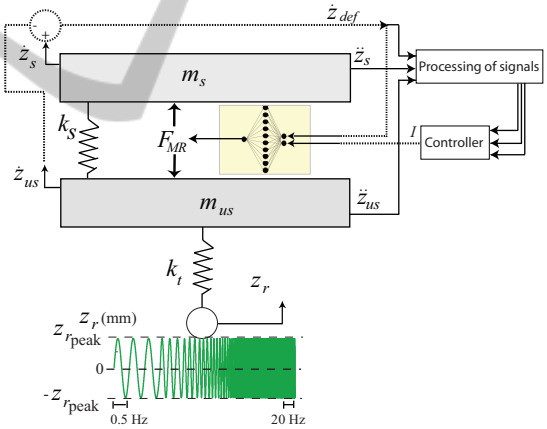

Figure 11: General structure of semiactive suspension control system.

In order to analyze the passengers comfort and road holding in the frequency and time domain, two road disturbance inputs have been simulated: 1) in the frequency domain, a signal chirp of 2 cm with span of [0.5-20]Hz and 2) in the time domain, a step of 3 cm. Figure 12 shows the *QoV* performance in the frequency domain; the Power Spectral Density (*PSD*) is used as performance index, i.e. the maximum gain of a signal is plotted at any specific frequency. The frequency response of the *QoV* model with the passive damper is considered as benchmark.

According to (Poussot-Vassal et al., 2008), Figure 12 shows that the controller fulfills with the per-

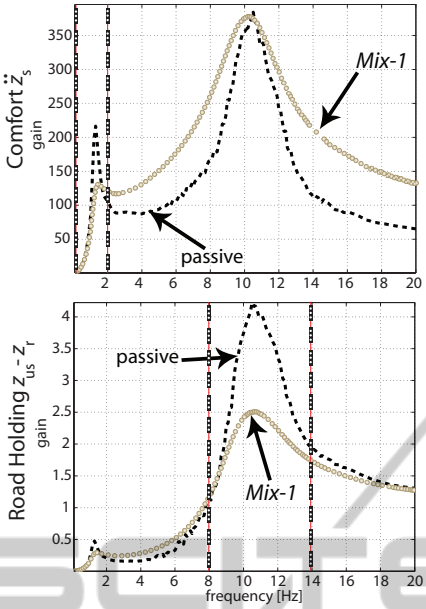

Figure 12: Frequency response of the *QoV* model in closed-loop using a semiactive and passive suspension, the span of frequencies of interest for each objective is bounded by the vertical discontinuous lines.

formance specification for comfort: at low frequencies [0-2]Hz, the maximum gain of $\ddot{z}_s$ respect to the surface is lower than the passive suspension. In this range of frequencies, a human can feel dizziness and sickness caused by sudden motions. On the other hand, a good road holding is considered when the maximum gain of $z_{us} - zr$ respect to z_r is limited to 2.5 for low disturbances ($z_r < 3cm$) between 0 to 20 Hz, specially close to the resonance frequency of m_{us}. Bottom plot in Figure 12 indicates that the semiactive suspension control system has good road holding performance in all span of frequencies, the *PSD* reduces until 2 units in the resonance frequency of the unsprung mass. Thus, the road holding increases 40.4% by using a semiactive suspension system.

For the time domain, the effectiveness of the semiactive suspension versus the passive suspension is clear. Figure 13 displays the transient response of the acceleration of the sprung mass (up plot) and of the wheel deflection (bottom plot). In both transient responses, the semiactive control system can reduce more of 50% in the settling time and decay ratio and approximately a 10% of the the maximum deviation, Table 8. Taking into account the *RMS* of the $\ddot{z}_s$ signal, the comfort increases 7.4% with the *Mix1* controller. For road holding, the *Mix1* controller improves 64.9% respect to he passive suspension.

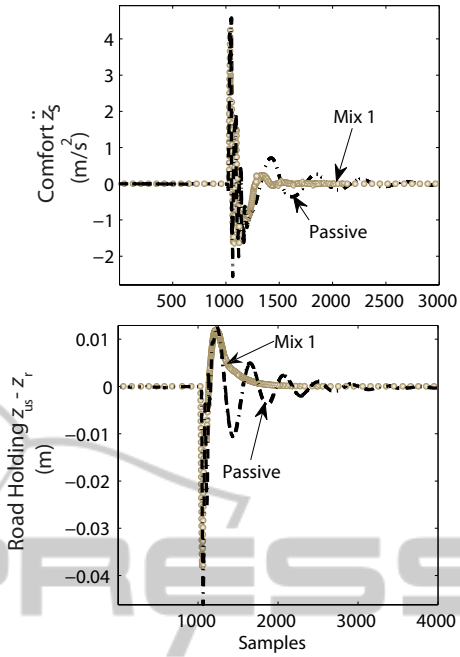

Figure 13: Transient response of the *QoV* model in closed-loop using different automotive suspension schemes.

Table 8: Performance in the transient response of the suspension control system.

Suspension Control System		Performance Index		
		Settling Time (s)	Decay Ratio	Maximum Deviation
Semi-active	Comfort	0.3	0.07	$4.1\frac{m}{s^2}$
	Holding	0.6	0	-3.8cm
Passive	Comfort	0.8	0.15	$4.5\frac{m}{s^2}$
	Holding	1.7	0.23	-4.5cm

6 CONCLUSIONS

A Magneto-Rheological (*MR*) damper model based on Artificial Neural Networks (*ANN*) is proposed. The *ANN* structure does not require regressors in the input vector and only one sensor (displacement or velocity) is demanded to get a reliable model. In addition, it has been proved that the output feedback in the input vector of the *ANN* model only improves slightly the modeling performance; however, the computing time in the training and testing step increases because the *ANN* architecture requires more model parameters when the output feedback is included.

Experimental data provided from two *MR* dampers (Delphi^{TM} named MR_1 damper, and BWI^{TM} named MR_2 damper) with different properties have been used to verify the accuracy of the proposed *MR* damper model based on *ANN*. The average modeling error in the force signal is lower than 7.25% by con-

sidering 5 different experiments. The force-velocity diagram shows that the MR_2 damper can be modeled with high accuracy by the proposed *ANN* structure since this shock absorber has an on/off actuation and does not have hysteresis; while the MR_1 damper presents a more complex dynamics at high frequencies with high displacements and the *MR* damper model based on the proposed 1-hidden layer structure can not represent this hysteretic behavior with only one sensor. However, this displacement pattern is out of the automotive operational zone of the damper, i.e. it does not occur at normal driving conditions.

By comparing the modeling performance of the proposed *MR* damper model based on *ANN* with another *MR* damper models presented in the literature, it is considerable to assume an optimal modeling performance. In the proposed *ANN* model, the obtained modeling error of 7.25% based on the *RMS* is equivalent to 4.7% of Error to Signal-Ratio (*ESR*), this means that the error in the proposed *ANN* model is: 1) lower than the *ESR* average (14.5%) obtained by the Bingham model and reported in (Savaresi et al., 2005); 2) lower than the *ESR* average (8.7%) obtained by a phenomenological model reported in (Ruiz-Cabrera et al., 2010); lower than the *ESR* average (38.7%) obtained by a semi-phenomenological model reported in (Ruiz-Cabrera et al., 2010); but greater than the *ESR* average of (0.9%) and (2%) obtained by an *ANN* model reported in (Savaresi et al., 2005) and (Ruiz-Cabrera et al., 2010) respectively. Although these latter *ANN* structures have regressors, use the output feedback and demand the displacement and velocity sensor.

Due to reliability of the proposed *MR* damper model and simplicity on the *ANN* structure, the model can be used to test semiactive suspension control systems. A control technique free of model has been used to control the semiactive suspension of a quarter of vehicle system; the performance of the passive suspension was used as benchmark. Simulation results show that passengers comfort and road holding can be increased at least 7.4% and 40.4% respectively, when an *MR* semiactive suspension is used.

ACKNOWLEDGEMENTS

Authors thank to CONACYT (Program of Postgraduate Cooperation - 2010) for the financial supports of this research.

REFERENCES

Ahn, K., Islam, M., and Truong, D. (2008). Hysteresis modeling of magneto-rheological (mr) fluid damper by self tuning fuzzy control. In *ICCAS 2008, Seoul Korea*, pages 2628–2633.

Atray, V. and Roschke, P. (2003). Design, fabrication, testing and fuzzy modeling of a large magneto-rheological damper for vibration control in a railcar. In *IEEE/ASME Joint Rail Conf.*, pages 223–229.

Boada, M., Calvo, J., Boada, B., and Díaz, V. (2011). Modeling of a magnetorheological damper by recursive lazy learning. *International Journal of Non-Linear Mechanics*, 46:479–485.

Çesmeci, S. and Engin, T. (2010). Modeling and testing of a field-controllable magnetorheological fluid damper. *International Journal of Mechanical Sciences*, 52(8):1036–1046.

Chang, C. and Zhou, L. (2002). Neural network emulation of inverse dynamics for a magnetorheological damper. *Journal of Structural Engineering*, 128(2):231–239.

Chen, E., Si, C., Yan, M., and Ma, B. (2009). Dynamic characteristics identification of magnetic rheological damper based on neural network. In *Artificial Intelligence and Computational Intelligence, 2009, Shangai, China*, pages 525–529.

Choi, S., Lee, S., and Park, Y. (2001). A hysteresis model for field-dependent damping force of a magnetorheological damper. *J. of Sound and Vibration*, 245(2):375–383.

Dong, X., Yu, M., Liao, C., and Chen, W. (2010). Comparative research on semi-active control strategies for magneto-rheological suspension. *Nonlinear Dynamics*, 59:433–453.

Du, H., Szeb, K., and Lam, J. (2005). Semiactive h_1 control of vehicle suspension with magneto-rheological dampers. *J. of Sound and Vibration*, 283:981–996.

Freeman, J. and Skapura, D. (1991). *Neural Networks: Algorithms, Applications and Programming Techniques*. Adisson-Wesley.

Gamota, D. and Filisko, F. (1991). Dynamic mechanical studies of electrorheological materials: Moderate frequencies. *Journal of Rheology*, 35:399–425.

Guo, S., Yang, S., and Pan, C. (2006). Dynamical modeling of magneto-rheological damper behaviors. *Int. Mater., Sys. and Struct.*, 16:3–14.

Hagan, M., Demuth, H., and Beale, M. (1996). *Neural Network Design*. PWS Publishing.

Hong, K., Sohn, H., and Hedrick, J. (2002). Modified skyhook control of semi-active suspensions: A new model, gain scheduling, and hardware-in-the-loop tuning. *J. Dyn. Sys., Meas., Control*, 124(1):158–167.

Korbicz, J., Koscielny, J., Kowalczuk, Z., and Cholewa, W. (2004). *Fault Diagnosis Models, Artificial Intelligence, Applications*. Springer.

Kwok, N., Ha, Q., Nguyen, T., Li, J., and Samali, B. (2006). A novel hysteretic model for magnetorheological fluid dampers and parameter identification using particle

swarm optimization. *Sensors and Actuators A: Physical*, 132:441–451.

Lozoya-Santos, J., Morales-Menendez, R., and Ramirez-Mendoza, R. (2009). Design of experiments for mr damper modelling. In *17th Int. Joint Conf. on Neural Networks*, pages 1915–1922.

Metered, H., Bonello, P., and Oyadiji, S. (2010). The experimental identification of magnetorheological dampers and evaluation of their controllers. *Mechanical Systems and Signal Processing*, 24:976–994.

Poussot-Vassal, C., Sename, O., Dugard, L., Gáspár, P., Szabó, Z., and Bokor, J. (2008). A new semi-active suspension control strategy through lpv technique. *Control Engineering Practice*, 16(12):1519–1534.

Ruiz-Cabrera, J., Díaz-Salas, V., Morales-Menendez, R., nón, L. G.-C., and Ramirez-Mendoza, R. (2010). Comparison of mr damper models. In *18th Mediterranean Conference on Control and Automation, Marrakech Morocco, June 23-25*, pages 1509–1513.

Savaresi, S., Bittanti, S., and Montiglio, M. (2005). Identification of semi-physical and black-box non-linear models: the case of mr-dampers for vehicles control. *Automatica*, 41:113–127.

Sjöberg, J. (1995). *Non-linear System Identification with Neural Networks*. PhD thesis, Linköping University, Sweden.

Spelta, M., Savaresi, S., and Fabbri, L. (2010). Experimental analysis of a motorcycle semi-active rear suspension. *Control Engineering Practice*, article in press:doi:10.1016/j.conengprac.2010.02.006.

Spencer, B., Dyke, S., Sain, M., and Carlson, J. (1996). Phenomenological model of a mr damper. *ASCE Journal of Engineering Mechanics*, 123(3):230–238.

Stanway, R., Sproston, J., and Stevens, N. (1987). Non-linear modeling of an electrorheological vibration damper. *Journal of Electrostatics*, 20:167–184.

Wang, L. and Kamath, H. (2006). Modeling hysteretic behaviour in mr fluids and dampers using phase-transition theory. *Smart Mater. Struct.*, 15:1725–1733.

Yang, G., Jr., B. S., and Dyke, S. (2002). Large-scale mr fluid dampers: Modeling and dynamic performance considerations. *Engineering Structures*, 24:309–323.

Zapateiro, M., Luo, N., Karimi, H., and Vehí, J. (2009). Vibration control of a class of semiactive suspension system using neural network and backstepping techniques. *Mechanical Systems and Signal Processing*, 23:1946–1953.